ISSN: 2458-8156

Journal Home page : http://dergipark.ulakbim.gov.tr/ejens * E-mail : editor@cnrgroup.eu

hosted by Turkish JournalPark ACADEMIC

EJENS

European Journal of Engineering and Natural Sciences CODEN: EJENS

Analysis Of Laminated Composite Plates Using Element-Free Galerkin Method

Omer Yavuz Bozkurt[1]*, Ozkan Ozbek[2]

[1]*Gaziantep University, Mechanical Engineering Department, 27310, Şehitkamil/Gaziantep, Turkey.*

[2]*Gaziantep University, Mechanical Engineering Department, 27310, Şehitkamil/Gaziantep, Turkey.*

**Corresponding Author email: oybozkurt@gantep.edu.tr*

Publication Info

Paper received:
10 December 2015

Revised received:
15 December 2015

Accepted:
18 December 2015

Abstract

The desire to use materials with high strength/weight or stiffness/weight ratio is increased the importance of composite materials nowadays. Due to this, much attention has been devoted to the numerical analysis of composite plates. The performance of well-known numerical methods, Finite Element Method (FEM) and Boundary Element Method (BEM), are based on the quality mesh structures. Meshfree methods are free from the meshes and the drawbacks of mesh-based interpolation techniques. Because of its high convergence rate, Element-Free Galerkin Method (EFGM) is one of the most widely used meshfree method in solid body mechanics and it is a promising candidate for the analysis of composite materials. In this study; deflection analysis of laminated composite plates are studied using EFGM. Several laminated composite plate problems are solved using EFGM and the displacement results of EFGM solutions are compared with the results of exact and FEM solutions at the critical points.

Key words

Laminate, composite plate, element-free Galerkin method, meshfree methods

1. INTRODUCTION

Nowadays, composite materials have played an important role in the engineering applications that require high strength/weight or stiffness/weight ratios. Because of that, analysis of composite materials have gained great significance. Several plate theories are present for the bending analysis of composite plates in the literature such as are Classical Plate Theory (CLPT) [1], First Order Shear Deformation Theory (FSDT) [1], Higher Order Shear Deformation Theory (HSDT) [1] etc. The FSDT, also known as Mindlin-Reissner plate theory, is widely used since it includes transverse shear effects and its simplicity.

Due to the complex structure of composite materials, several numerical methods, such as FEM, BEM and meshfree methods, have been used for the analyses of composite laminates in the literature. Sheikh et al. [2] used FEM on the solution of composite plates having different shapes. Moments and stresses using BEM were examined by Albuquerque and his friends [3]. Haddad et al. [4] applied to Finite Difference Method (FDM) for free vibration analysis of composite plates.

The performances of FEM and BEM depend on mesh quality of the problem model. Meshfree methods have been developed to overcome this limitation. Element-Free Galerkin Method (EFGM), which was originally developed by Belytschko [5], is one of the most widely used meshfree method in solid mechanics due to its simplicity and high convergence rate. Also, many scientists propose that EFGM has good solution accuracy in solid mechanics [6]. The EFGM is seen as a promising candidate for the analysis of composite materials. It was used by Belinha and Dinis for the analysis of anisotropic plates and laminates [7]. Also, EFGM has been preferred for the various analysis of

composite plates such as buckling problems [8], vibration problems [9], bending problems [7], crack analysis [10], fracture analysis [11], etc.

In this study, EFGM and FEM programs, based on FSDT, have been written on MATLAB programming environment for the deflection analysis of laminated composite plates. Several numerical examples are solved using particular number of nodes in the problem domain. The displacement results of EFGM are presented and compared with the results of FEM and exact solution in terms of accuracy.

2. FIRST SHEAR DEFORMATION THEORY (FSDT) FOR THE LAMINATED COMPOSITE PLATES

A typical Mindlin-Reissner plate with mid-plane lying in the x-y plane of Cartesian coordinate system is depicted in Fig 1. The displacement field of a point at a distance z to the mid-plane can be written as

$$\mathbf{u} = \begin{Bmatrix} u \\ v \\ w \end{Bmatrix} = \begin{Bmatrix} -z\theta_x(x,y) \\ -z\theta_y(x,y) \\ w(x,y) \end{Bmatrix} \tag{1}$$

where (u, v, w) are the displacements of the plate in the x, y, z directions. θ_x and θ_y are the rotations of cross-section of the plate about y and x axes, respectively. The linear strains in the Mindlin-Reissner plate are the strains resulting from bending are obtained in terms of the rotations, θ_x, θ_y and of the mid-surface displacement, w, as

$$\boldsymbol{\varepsilon} = \begin{Bmatrix} \varepsilon_{xx} \\ \varepsilon_{yy} \\ \gamma_{xy} \\ \gamma_{yz} \\ \gamma_{xz} \end{Bmatrix} = \begin{Bmatrix} -z\frac{\partial\theta_x(x,y)}{\partial x} \\ -z\frac{\partial\theta_y(x,y)}{\partial y} \\ -z\frac{\partial\theta_x(x,y)}{\partial y} - z\frac{\partial\theta_y(x,y)}{\partial x} \\ -\theta_y(x,y) + \frac{\partial w(x,y)}{\partial y} \\ -\theta_x(x,y) + \frac{\partial w(x,y)}{\partial x} \end{Bmatrix} \tag{2}$$

Using the generalized Hooke's law for orthotropic linear elastic materials, the stresses for the i^{th} layer is given as,

$$\boldsymbol{\sigma}^i = \bar{\mathbf{c}}^i\boldsymbol{\varepsilon} \tag{3}$$

where

$$\boldsymbol{\sigma}^i = \{\sigma_{xx} \quad \sigma_{yy} \quad \tau_{xy} \quad \tau_{yz} \quad \tau_{xz}\}^T \tag{4}$$

$$\bar{\mathbf{c}}^i = \mathbf{T}^T\mathbf{c}^i\mathbf{T} \tag{5}$$

where $\mathbf{c}^i$ is the material matrix of the i^{th} layer. It includes six independent material properties that are E_1, E_2, ϑ_{12}, G_{12}, G_{13} and G_{23},. The material matrix of the orthotropic materials can be written as

$$\mathbf{c}^i = \begin{bmatrix} \frac{E_1}{1-\nu_{12}\nu_{21}} & \frac{E_1\nu_{21}}{1-\nu_{12}\nu_{21}} & 0 & 0 & 0 \\ \frac{E_1\nu_{12}}{1-\nu_{12}\nu_{21}} & \frac{E_2}{1-\nu_{12}\nu_{21}} & 0 & 0 & 0 \\ 0 & 0 & G_{12} & 0 & 0 \\ 0 & 0 & 0 & G_{23} & 0 \\ 0 & 0 & 0 & 0 & G_{31} \end{bmatrix} \tag{6}$$

and $\mathbf{T}$ is the transformation matrix, which has lay-up of the laminae, can be given as

$$\mathbf{T} = \begin{bmatrix} \cos^2\theta & \sin^2\theta & -\sin 2\theta & 0 & 0 \\ \sin^2\theta & \cos^2\theta & \sin 2\theta & 0 & 0 \\ \sin\theta\cos\theta & -\sin\theta\cos\theta & \cos^2\theta - \sin^2\theta & 0 & 0 \\ 0 & 0 & 0 & \cos\theta & -\sin\theta \\ 0 & 0 & 0 & \sin\theta & \cos\theta \end{bmatrix} \tag{7}$$

where the θ is the lay-up or orientation of fiber on the i^{th} lamina.

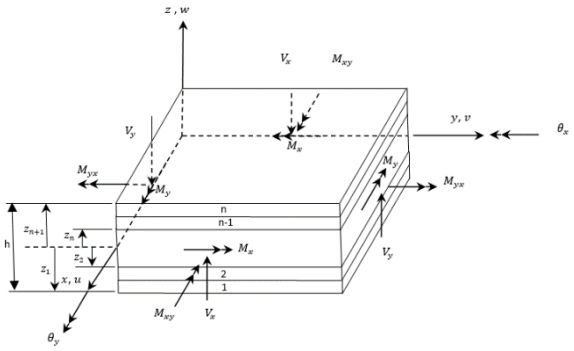

Figure 1. A typical laminate plate

Considering the $\{\varepsilon_{xx}\ \ \varepsilon_{yy}\ \ \gamma_{xy}\} = z\,\{\bar{\varepsilon}_{xx}\ \ \bar{\varepsilon}_{yy}\ \ \bar{\gamma}_{xy}\}$ the stresses on the top face of layer (i) are

$$\begin{aligned}
\sigma_{xx}^{z_i+1} &= z_{i+1}\left[\bar{c}_{11}{}^{i}\,\bar{\varepsilon}_{xx} + \bar{c}_{12}{}^{i}\,\bar{\varepsilon}_{yy} + \bar{c}_{13}{}^{i}\,\bar{\gamma}_{xy}\right]\\
\sigma_{yy}^{z_i+1} &= z_{i+1}\left[\bar{c}_{12}{}^{i}\,\bar{\varepsilon}_{xx} + \bar{c}_{22}{}^{i}\,\bar{\varepsilon}_{yy} + \bar{c}_{23}{}^{i}\,\bar{\gamma}_{xy}\right]\\
\tau_{xy}^{z_i+1} &= z_{i+1}\left[\bar{c}_{13}{}^{i}\,\bar{\varepsilon}_{xx} + \bar{c}_{23}{}^{i}\,\bar{\varepsilon}_{yy} + \bar{c}_{33}{}^{i}\,\bar{\gamma}_{xy}\right]\\
\tau_{xz}^{z_i+1} &= \left[\bar{c}_{44}{}^{i}\,\gamma_{xz} + \bar{c}_{45}{}^{i}\,\gamma_{yz}\right]\\
\tau_{yz}^{z_i+1} &= \left[\bar{c}_{45}{}^{i}\,\gamma_{xz} + \bar{c}_{55}{}^{i}\,\gamma_{yz}\right]
\end{aligned} \tag{8}$$

The bending moments (M_{ij}) and the shear forces (V_{ij})are

$$\begin{aligned}
M_{xx} &= \sum_i^n \int_{z_i}^{z_i+1} z\,\sigma_{xx}^i dz\\
M_{yy} &= \sum_i^n \int_{z_i}^{z_i+1} z\,\sigma_{yy}^i dz\\
M_{xy} &= \sum_i^n \int_{z_i}^{z_i+1} z\,\tau_{xy}^i dz
\end{aligned} \tag{9}$$

and

$$\begin{aligned}
V_{xx} &= k_{sh}\sum_i^n \int_{z_i}^{z_i+1} \tau_{xz}^i dz\\
V_{yy} &= k_{sh}\sum_i^n \int_{z_i}^{z_i+1} \tau_{yz}^i dz
\end{aligned} \tag{10}$$

where k_{sh} is the shear correction factor. Substituting the stress values in Eqs. (8) into moment in Eqs. (9) and shear forces in Eqs. (10):

$$\begin{aligned}
M_{xx} &= \sum_i^n \left[\frac{z_{i+1}^3}{3} - \frac{z_i^3}{3}\right]\left[\bar{c}_{11}{}^{i}\,\bar{\varepsilon}_{xx} + \bar{c}_{12}{}^{i}\,\bar{\varepsilon}_{yy} + \bar{c}_{13}{}^{i}\,\bar{\gamma}_{xy}\right]\\
M_{yy} &= \sum_i^n \left[\frac{z_{i+1}^3}{3} - \frac{z_i^3}{3}\right]\left[\bar{c}_{12}{}^{i}\,\bar{\varepsilon}_{xx} + \bar{c}_{22}{}^{i}\,\bar{\varepsilon}_{yy} + \bar{c}_{23}{}^{i}\,\bar{\gamma}_{xy}\right]\\
M_{xy} &= \sum_i^n \left[\frac{z_{i+1}^3}{3} - \frac{z_i^3}{3}\right]\left[\bar{c}_{13}{}^{i}\,\bar{\varepsilon}_{xx} + \bar{c}_{12}{}^{i}\,\bar{\varepsilon}_{yy} + \bar{c}_{13}{}^{i}\,\bar{\gamma}_{xy}\right]\\
V_{xx} &= k_{sh}\sum_i^n [z_{i+1} - z_i]\left[\bar{c}_{44}{}^{i}\,\gamma_{xz} + \bar{c}_{45}{}^{i}\,\gamma_{yz}\right]\\
V_{yy} &= k_{sh}\sum_i^n [z_{i+1} - z_i]\left[\bar{c}_{45}{}^{i}\,\gamma_{xz} + \bar{c}_{55}{}^{i}\,\gamma_{yz}\right]
\end{aligned} \tag{11}$$

The Eqs. (11) can be arranged as in the following form:

$$\mathbf{M} = \begin{bmatrix} M_{xx} \\ M_{yy} \\ M_{xy} \end{bmatrix} = \sum_i^n \mathbf{D}^i \mathbf{L} \Phi \left(\frac{z_{i+1}^3}{3} - \frac{z_i^3}{3}\right) = \left[\sum_i^n \mathbf{D}^i \left(\frac{z_{i+1}^3}{3} - \frac{z_i^3}{3}\right)\right] \mathbf{L}\Phi$$

$$\mathbf{V} = \begin{bmatrix} V_{xx} \\ V_{yy} \end{bmatrix} = k_{sh}\sum_i^n [\mathbf{A}_{sh}^i(\nabla \mathbf{w} - \Phi)(z_{i+1} - z_i)] = k_{sh}\,[\sum_i^n \mathbf{A}_{sh}^i (z_{i+1} - z_i)](\nabla \mathbf{w} - \Phi) \tag{12}$$

where,

$$\mathbf{L} = \begin{bmatrix} -\frac{\partial}{\partial x} & 0 & -\frac{\partial}{\partial y} \\ 0 & -\frac{\partial}{\partial y} & -\frac{\partial}{\partial x} \end{bmatrix} \tag{13}$$

$$\Phi = \{\theta_x \quad \theta_y\}^T \tag{14}$$

$$\nabla = \left\{\frac{\partial}{\partial x} \quad \frac{\partial}{\partial y}\right\}^T \tag{15}$$

and $\mathbf{D}^i$and $\mathbf{A}_{sh}^i$are the material properties related with bending and shear effects. They can be written in the matrix forms, as follows:

$$\mathbf{D}^i = \begin{bmatrix} \bar{c}_{11}{}^i & \bar{c}_{12}{}^i & \bar{c}_{13}{}^i \\ \bar{c}_{12}{}^i & \bar{c}_{22}{}^i & \bar{c}_{23}{}^i \\ \bar{c}_{13}{}^i & \bar{c}_{23}{}^i & \bar{c}_{33}{}^i \end{bmatrix} \tag{16}$$

$$\mathbf{A}_{sh}^i = \begin{bmatrix} \bar{c}_{44}{}^i & \bar{c}_{45}{}^i \\ \bar{c}_{45}{}^i & \bar{c}_{55}{}^i \end{bmatrix} \tag{17}$$

In the absence of mass forces, the equilibrium equations obtained using the virtual work principle are given as,

$$\begin{aligned} \mathbf{L}^T\mathbf{M} - \mathbf{V} &= 0 \\ \nabla^T\mathbf{V} + \mathbf{b} &= 0 \end{aligned} \tag{18}$$

where $\mathbf{b}$ is the vector of applied external forces. EFGM is used for the solution of this system equations.

3. ELEMENT-FREE GALERKIN METHOD

3.1. Moving-Least Square (MLS) Approximation

The MLS approximation for the function of a field variable $u(\mathbf{x})$ in a local domain Ω is defined at a point $\mathbf{x}$ as

$$u^h(\mathbf{x}) = \sum_{i=1}^{m} p_i(\mathbf{x})a_i(\mathbf{x}) = \mathbf{p}^T(\mathbf{x})\mathbf{a}(\mathbf{x}) \tag{19}$$

where m is the number of basis terms, $\mathbf{p}^T(\mathbf{x}) = \{p_1(\mathbf{x}), p_2(\mathbf{x}), p_3(\mathbf{x}), \cdots, p_m(\mathbf{x})\}$ is the vector of monomial basis functions, $\mathbf{a}^T(\mathbf{x}) = \{a_1(\mathbf{x}), a_2(\mathbf{x}), a_3(\mathbf{x}), \cdots, a_m(\mathbf{x})\}$ is the vector of coefficients, and $\mathbf{x}^T = [x, y]$ is the position vector for 2D problems. The monomials are selected from the Pascal triangle with providing minimum completeness to build the basis function $\mathbf{p}^T(\mathbf{x})$. For example, the linear and quadratic basis functions in 2D problems can be given by

$$\mathbf{p}^T(\mathbf{x}) = [1, x, y], \qquad m = 3 \tag{20}$$

$$\mathbf{p}^T(\mathbf{x}) = [1, x, y, x^2, xy, y^2], \qquad m = 6 \tag{21}$$

The difference between the function $u(\mathbf{x})$ and its local approximation $u^h(\mathbf{x})$ must be minimized by weighted discrete L_2 norm to obtain the vector of coefficients $\mathbf{a}(\mathbf{x})$.

$$J = \sum_{i=1}^{n} w(\mathbf{x} - \mathbf{x}_i)[\mathbf{p}^T(x_i)\mathbf{a}(\mathbf{x}) - u_i]^2 \tag{22}$$

where n is the number of nodes in the support domain of point $\mathbf{x}$, u_i is the nodal value of u at $\mathbf{x} = x_i$, $w(\mathbf{x} - x_i)$ is the weight function associated with the influence domain of node i. From weight function properties, it must be greater than zero for all nodes in the support domain of point $\mathbf{x}$.

The minimization of weighted residual with respect to $\mathbf{a}(\mathbf{x})$ at any arbitrary point $\mathbf{x}$ gives

$$\frac{\partial J}{\partial \mathbf{a}} = 0 \tag{23}$$

which can be written as a set of linear equations.

$$\mathbf{A}(\mathbf{x})\mathbf{a}(\mathbf{x}) = \mathbf{B}(\mathbf{x})\mathbf{U}_s \tag{24}$$

where $\mathbf{U}_s = \{u_1, u_2, u_3, \cdots, u_n\}^T$ is the vector of nodal values of field function for the nodes of support domain. The matrices $\mathbf{A}$ and $\mathbf{B}$ have the following forms

$$\mathbf{A}(\mathbf{x}) = \sum_{i=1}^{n} w_i(\mathbf{x})p(x_i)p^T(x_i), \qquad w_i(\mathbf{x}) = w(\mathbf{x} - x_i) \tag{25}$$

$$\mathbf{B}(\mathbf{x}) = [w_1(\mathbf{x})p(x_1) \quad w_2(\mathbf{x})p(x_2) \quad \cdots \quad w_n(\mathbf{x})p(x_n)] \tag{26}$$

The matrix $\mathbf{A}$ is called as weighted moment matrix of MLS and if it is non-singular $\mathbf{a}(\mathbf{x})$ can be written as

$$\mathbf{a}(\mathbf{x}) = \mathbf{A}^{-1}(\mathbf{x})\mathbf{B}(\mathbf{x})\mathbf{U}_s \tag{27}$$

The local approximation $u^h(\mathbf{x})$ can be rewritten by substituting Eq. (19)

$$u^h(\mathbf{x}) = \sum_{i=1}^{n} \phi_i(\mathbf{x})u_i = \mathbf{\Phi}^T(\mathbf{x})\mathbf{U}_S \tag{28}$$

where $\mathbf{\Phi}^T$is the vector of MLS shape functions and it can be expressed as

$$\mathbf{\Phi}^T(x) = \{\phi_1(x) \quad \phi_2(x) \quad \cdots \quad \phi_n(x)\} = \mathbf{p}^T(x)\mathbf{A}^{-1}(x)\mathbf{B}(x) \tag{29}$$

The partial derivatives of shape function can be achieved by the following equation.

$$\Phi_{,i} = (\mathbf{p}^T\mathbf{A}^{-1}\mathbf{B})_{,i} = \mathbf{p}_{,i}^T\mathbf{A}^{-1}\mathbf{B} + \mathbf{p}^T\mathbf{A}_{,i}^{-1}\mathbf{B} + \mathbf{p}^T\mathbf{A}^{-1}\mathbf{B}_{,i} \tag{30}$$

where

$$\mathbf{A}_{,i}^{-1} = -\mathbf{A}^{-1}\mathbf{A}_{,i}\mathbf{A}^{-1} \tag{31}$$

The spatial derivative are designated with index i following a comma. The weight functions are one of the most important points for derivation of MLS shape functions. The continuity and locality features of the MLS approximation are mainly based on weight functions. The weight function must be positive inside the support domain by taking its maximum value at the centre of support domain and must be zero outside the support domain using a monotonically decrease. There are various weight functions in literature [6]. The cubic spline weight function is used in this work and is given by

$$w_i(\mathbf{x} - x_i) = w(\bar{r_i}) = \begin{cases} 2/3 - 4\bar{r_i}^2 + 4\bar{r_i}^3 & \bar{r_i} \le 0.5 \\ 4/3 - 4\bar{r_i} + 4\bar{r_i}^2 - 4/3\,\bar{r_i}^3 & 0.5 < \bar{r_i} \le 1 \\ 0 & \bar{r_i} > 1 \end{cases} \tag{32}$$

For rectangular influence domain in 2-D problems, weight functions can be obtained by

$$w(\bar{r_i}) = w(r_x)w(r_y) = w_x w_y \tag{33}$$

$$r_x = \frac{|x - x_i|}{r_{wx}} \quad \text{and} \quad r_y = \frac{|y - y_i|}{r_{wy}} \tag{34}$$

where r_{wx} and r_{wy} are the size of support domain in the x and y direction.

3.2. Galerkin Weak Form and Enforcement Boundary Conditions

The Galerkin weak form for Mindlin-Reissner plates can written as

$$\int_\Omega \delta(\mathbf{L}_d u)^T D L_d u d\Omega - \int_\Omega \delta(\mathbf{L}_u u)^T b d\Omega - \int_{\Gamma_t} \delta(\mathbf{L}_u u)^T t_\Gamma dS + \delta \int_{\Gamma_u} \frac{1}{2}(u_b - u_\Gamma)^T \alpha (u_b - u_\Gamma) d\Gamma = 0 \tag{35}$$

The discrete system equation can be written as

$$(\mathbf{K} + \mathbf{K}^\alpha)\mathbf{U} = (\mathbf{F} + \mathbf{F}^\alpha) \tag{36}$$

where **K** is the global stiffness matrix and is obtained by assembling the point stiffness matrices

$$K_{ij} = \int_\Omega \mathbf{B}_i^T \mathbf{D} \mathbf{B}_j d\Omega \tag{37}$$

in which

$$\mathbf{B}_i = \begin{bmatrix} 0 & 0 & 0 & \frac{\partial \phi_i}{\partial x} & \frac{\partial \phi_i}{\partial y} \\ \frac{\partial \phi_i}{\partial x} & 0 & \frac{\partial \phi_i}{\partial y} & \phi_i & 0 \\ 0 & \frac{\partial \phi_i}{\partial y} & \frac{\partial \phi_i}{\partial x} & 0 & \phi_i \end{bmatrix}^T \tag{38}$$

and the $\mathbf{K}^\alpha$is the matrix of penalty factors defined by

$$(\mathbf{K}^\alpha)_{ij} = \int_{\Gamma_u} \varphi_i^T \boldsymbol{\alpha} \varphi_j d\Gamma \tag{39}$$

where φ_i is a diagonal matrix. If the relevant DOF is free, the diagonal elements of φ_i are equal to 0, otherwise equal to 1.

The force vector **F** in Eq. (35) is the global force vector assembled using the nodal force vector of

$$F_i = \int_\Omega (\mathbf{L}_u \Phi_i)^T b d\Omega + \int_\Omega (\mathbf{L}_u \Phi_i)^T t_\Gamma dS \tag{40}$$

where Φ_i is a diagonal matrix of shape functions.

The $\mathbf{F}^{\alpha}$ vector shows the forces obtained by the implementation of essential boundary conditions and can be obtained as follows

$$F_i^{\alpha} = \int_{\Gamma_u} \varphi_i{}^T \alpha u_{\Gamma} d\Gamma \quad (41)$$

4. NUMERICAL RESULTS AND DISCUSSIONS

In this section, a few numerical examples have been performed to demonstrate the applicability and the accuracy of the EFGM. Plates with boundary conditions, thickness ratios, number of layers, fiber orientations and materials are studied. The results are provided in terms of normalized displacements for the convenience of comparison and validated by comparing them with analytical results taken from the literature and FEM results. The behaviour of all composite materials used is considered as linear elastic. The value of shear correction factor is constant and taken as $5/6$ for all examples. The properties of materials used in the examples are given in Table 1. The linear polynomial basis, cubic spline weight function, 2.5 for the dimensionless support domain size and 7×7 Gauss quadrature integration points are used in all EFGM solutions.

Table 1. Properties of laminated composite plates

	M1	**M2**	**M3**
$\boldsymbol{E1}, Pa$	250×10^9	40×10^6	300×10^9
$\boldsymbol{E2}, Pa$	10×10^9	1.0×10^6	12×10^9
$\boldsymbol{G_{12}}, Pa$	5×10^9	0.6×10^6	6×10^9
$\boldsymbol{G_{13}}, Pa$	5×10^9	0.6×10^6	6×10^9
$\boldsymbol{G_{23}}, Pa$	2×10^9	0.5×10^6	2.4×10^9
$\boldsymbol{v_{12}}$	0.25	0.25	0.25

4.1. Simply supported laminated composite plates under uniformly distributed load

The deformation of a simply supported square laminated plate subjected to a uniformly distributed transverse load $q = 100$ kN/m^2 is analysed using different lamination schemes with thickness/span ratios of $h/L = 0.1, h/L = 0.05$ and $h/L = 0.01$. The laminates used are orthotropic laminate with one layer of [0°] orientation, symmetric cross-plies with three, four, five and seven layers of [0°/90°/0°], [0°/90°/90°/0°], [0°/90°/0°90°/0°] and [0°/90°/90°/0°/90°/90°/0°] orientations, respectively. The material M1, presented in Table 1, is used in this example.

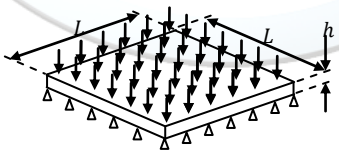

Figure 2. Simply supported laminated composite square plate

Due to the symmetry, only a quarter of plate is modelled using 441 nodes in the EFGM and FEM solutions. The dimensionless center deflection of plate is presented in Table 2. It can be seen that the accuracy of EFGM solution is near to the exact solution and is better than the FEM.

Table 2. Central deflections $100wE_2h^3/(qL^4)$ *under uniform transverse load*

h/L	Lay-up	FEM	EFGM	Exact [12]
0.01	0	0.662553	0.659729	0.6528
	0/90/0	0.680383	0.677547	0.6697
	0/90/90/0	0.694267	0.691600	0.6833
	0/90/0/90/0	0.698297	0.695732	0.6874
	0/90/90/0/90/90/0	0.701414	0.698928	0.6896
0.05	0	0.737233	0.734517	0.7262
	0/90/0	0.769471	0.766675	0.7572
	0/90/90/0	0.781553	0.778914	0.7694
	0/90/0/90/0	0.769781	0.767292	0.7581
	0/90/90/0/90/90/0	0.767333	0.764929	0.7575
0.1	0	0.966699	0.963153	0.9519
	0/90/0	1.038240	1.034393	1.0219
	0/90/90/0	1.040156	1.036504	1.0250
	0/90/0/90/0	0.986117	0.982779	0.9727
	0/90/90/0/90/90/0	0.969344	0.966131	0.9643

4.2. Simply supported angle-ply square plate under uniformly distributed load

The deformation of an angle-ply simply supported square plate subjected to a uniformly distributed transverse load $q = 1$ is examined using four layers $[\theta°/-\theta°/\theta°/-\theta°]$. The solutions are presented with a constant thickness-to-span ratio, h / L, of 0.1. The material M2 is used in this example.

Because of the asymmetry, the whole plate is modelled using 441 nodes in the EFGM and FEM solutions. Table 3 presents the dimensionless center deflection of plate. It is visible that the accuracy of EFGM solution is more accurate than the FEM. Also, it can be achieved to exact results by particular number of nodes used in the solution.

Table 3. Central deflections $100wE_2h^3/(qL^4)$ *under uniform transverse load*

Arrangement of layers $[\theta°/-\theta°/\theta°/-\theta°]$	FEM	EFGM	Exact [12]
-5/+5/-5/+5	6.922555	6.892311	6.741
-15/+15/-15/+15	6.205659	6.180749	6.086
-30/+30/-30/+30	4.841598	4.820746	4.825
-45/+45/-45/+45	4.430046	4.410081	4.426

4.3. Clamped laminated composite plates under uniformly distributed load

Clamped laminated square plate with four different aspect ratios of $h / L = 0.1, h / L = 0.05, h / L = 0.02$ and $h / L = 0.01$ are analyzed to determine deformations under the uniformly distributed transverse load $q = 1$. The unidirectional laminate of material M3 is used with four layer of $[0°/90°/90°/0°]$ orientation. Due to the symmetry, only a quarter of plate is modelled using 441 nodes in the EFGM and FEM solutions. The dimensionless center deflection of plate is presented in Table 4. A close agreement between the results of EFGM and exact solution is shown for all thickness ratios examined. Again the results of EFGM is better than the FEM ones.

Table 4. Central deflections $100wE_2h^3/(qL^4)$ *under uniform transverse load*

h/L	FEM	EFGM	Exact [13]
0.1	0.465766	0.46542	0.4651
0.05	0.234185	0.234522	0.2342
0.02	0.158636	0.159152	0.159
0.01	0.147079	0.147363	0.1475

5. CONCLUSIONS

In this study, the EFGM based on First Order Shear Deformation Theory is successfully implemented in the bending analyses of laminated composite plates. The results for the analyzed plates are in good agreement with the results of exact solutions. It is also shown that the accuracy of EFGM solutions are better than the FEM ones for the analyzed plates.

REFERENCES

[1]. J. N. Reddy, A. A. Khdeir, "Buckling of vibration of laminated composite plates using various plate theories," *AIAA Journal*, 27(12), 1808-1817, 1989.
[2]. A. H. Sheikh, S. Haldar, D. Sengupta, "A high precision shear deformable element for the analysis of laminated composite plates of different shapes," *Composite Structures*, 55(3), 329-336, 2002.
[3]. A. Reis, E. L. Albuquerque, F. L. Torsani, L. P. Junior, P. Sollero, "Computation of moments and stresses in laminated composite plates by the boundary element method," *Engineering Analysis with Boundary Elements*, 35, 105-113, 2010.
[4]. S. K. Numayr, R. H. Haddad, M. A. Haddad, "Free vibration of composite plates using the finite difference method," *Thin-Walled Structures*, 42, 399-414, 2004.
[5]. T. Belytschko, "Meshless methods an overview and recent developments," *International Journal for Numerical Methods in Engineering*, 38, 1655-1679, 1996.
[6]. G.R. Liu, *Mesh Free Methods Moving Beyond The Finite Element Method*, Taylor and Francis Group, (2003).
[7]. J. Belinha, L. M. J. S. Dinis, "Analysis of plates and laminates using the element-free Galerkin method," *Computers and Structures*, 84, 1547-1559, 2006.
[8]. A. G. Arani, Sh. Maghamikia, M. Mohammadimehr, A. Arefmanesh, "Buckling analysis of laminated composite rectangular plates reinforced by SWCNTs using analytical and finite element methods," *Journal of Mechanical Science and Technology*, 25(3), 809-820, 2011.
[9]. M. R. Aagaah, M. Mahinfalah, G. N. Jazar, "Natural frequencies of laminated composite plates using third order shear deformation theory," *Composite Structures*, 72, 273-279, 2006.
[10]. S. S. Ghorashi, S. R. Sabbagh-Yazdi, S. Mohammadi, "Element free Galerkin method for crack analysis of orthotropic plates," *Computational Methods in Civil Engineering*, 1, 1-13, 2010.
[11]. S. S. Ghorashi, S. Mohammadi, S. R. Sabbagh-Yazdi, "Orthotropic enriched element free Galerkin method for fracture analysis of composites," *Engineering Fracture Mechanics*, 78, 1906-1927, 2011.
[12]. J. N. Reddy, *Mechanics of laminated composite plates*, CRC Press, 1996.
[13]. P. Umasree, K. Bhaskar, "Accurate flexural analysis of clamped moderately thick cross-ply rectangular plates by superposition of exact untruncated infinite series solutions," *Journal of Reinforced Plastics Composite*, 24(16), 1723-1736, 2002.